Effect of Multiple Substorms on the Ring Current

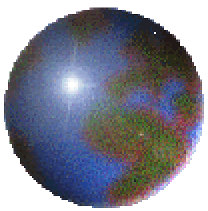

Kristi A. Keller, Ayris Falasca, Mei-Ching Fok, Michael Hesse, Lutz Rastaetter, Maria M. Kuznetsova

Goddard Space Flight Center

Tamas I. Gombosi, Darren L. DeZeeuw

University of Michigan

Abstract

The effect of magnetospheric substorms on the ring current is not completely understood. Using a combination of the University of Michigan's BAT-S-RUS Model and Mei-Ching Fok's Ring Current Model, we will study how substorms can affect the ring current. Using simulated solar wind to drive substorms, we will study the effects of multiple substorms on the ring current. In particular we will study how the symmetry and energy of the ring current are different for multiple substorms as compared to isolated substorms. We will also study how multiple substorms can drive injections into the ring current.

BATSRUS Information

- BATSRUS solves the ideal MHD equations using an adaptive mesh. In this run the smallest resolution was 1/8 R_E. After the initial setup, the grid was fixed.
- The box was from –255 to 33 R_E in the GSM x direction and –48 to 48 R_E in the other two directions.
- The FACs at 4 R_E are mapped along dipole field lines to the ionosphere to calculate the electrostatic potential in the ionosphere.

Fok Model

- The Fok Ring Current Model calculates the evolution of the ring current particle fluxes by solving a bounce-averaged Boltzmann transport equation.
- The model uses a combined drift-diffusion approach.
  - The particle drift terms include gradient-curvature drift and *E*x*B* drift (includes corotation and the ionospheric electric field).
  - The diffusion terms include radial and pitch angle diffusion.
- The model also calculates losses due to charge exchange.

Fok Model

- The Fok Ring Current Model uses the ionospheric potential and magnetic field from the BATSRUS model.
- The Fok Ring Current Model uses the density and temperature from the BATSRUS model at the Ring Current Model's outer boundary.
- The pitch-angle distribution at the model's outer boundary is assumed to be isotropic.
- For the initial source population, the energy distribution is assumed to be a Kappa distribution.

Run with Model Solar Wind Conditions Case 1

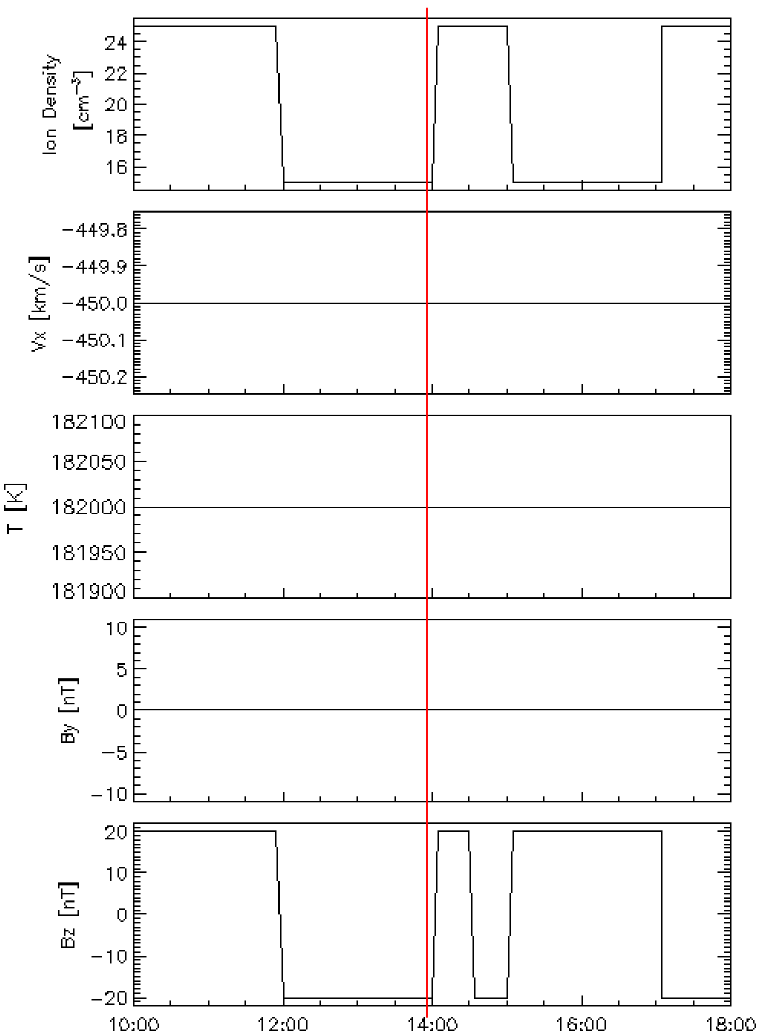

Hours

Cross Polar Cap Potential in Northern Hemisphere

ϕ (kV)

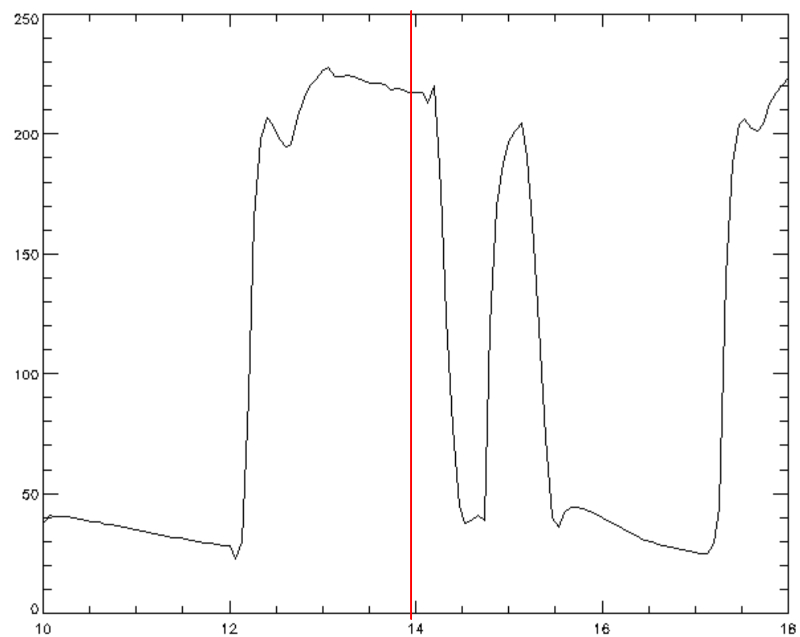

Universal Time (hours)

The period before the red line corresponds to a “warm-up” period for the ring current.

Magnetosphere Case 1

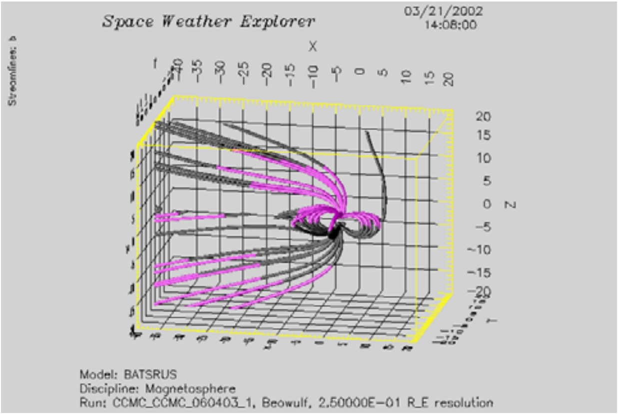

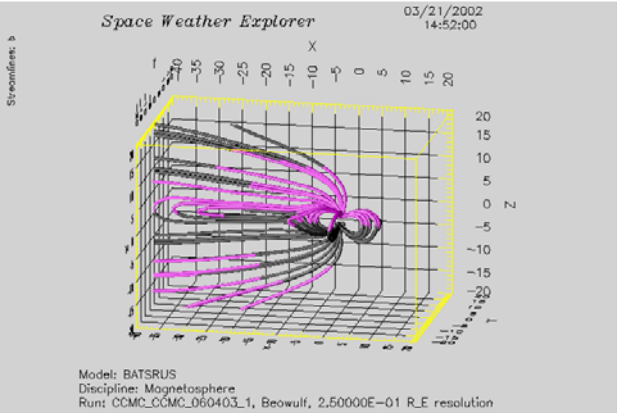

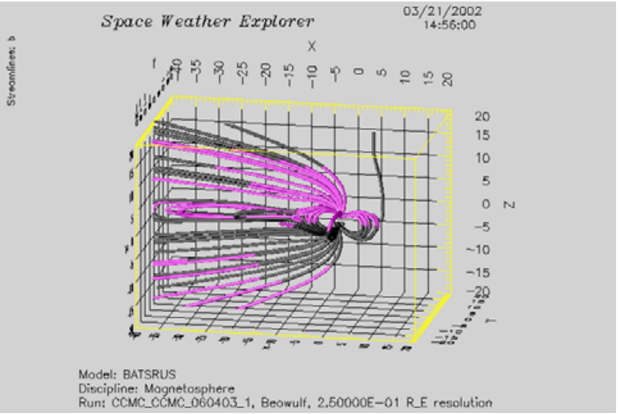

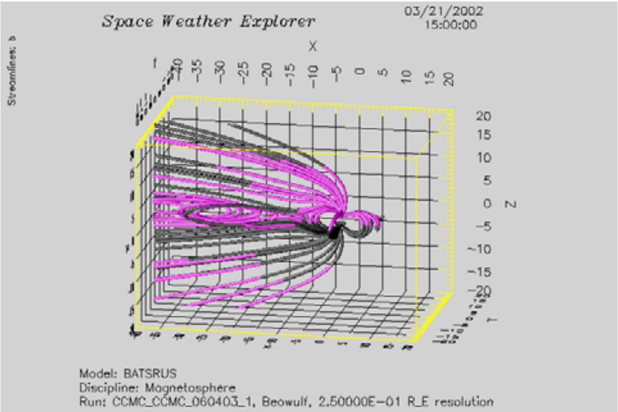

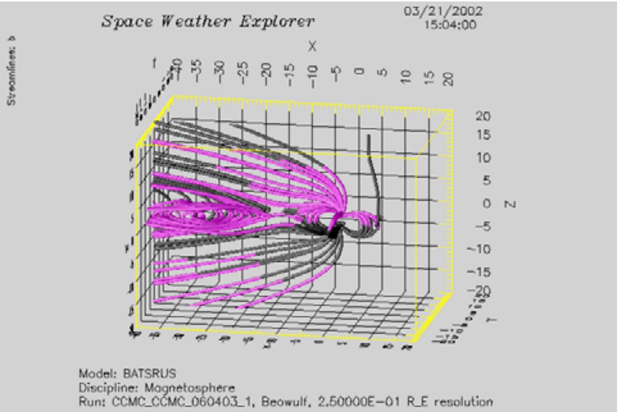

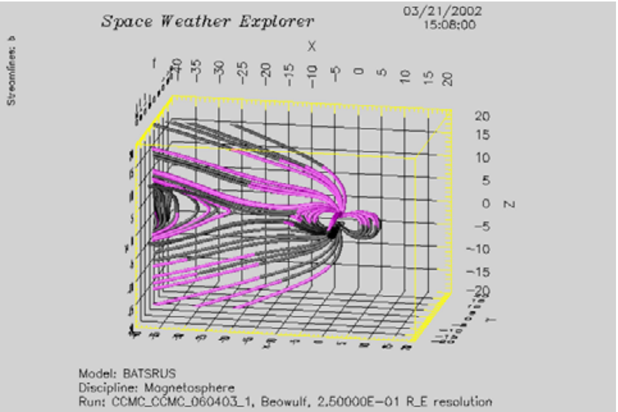

Magnetosphere Case 1

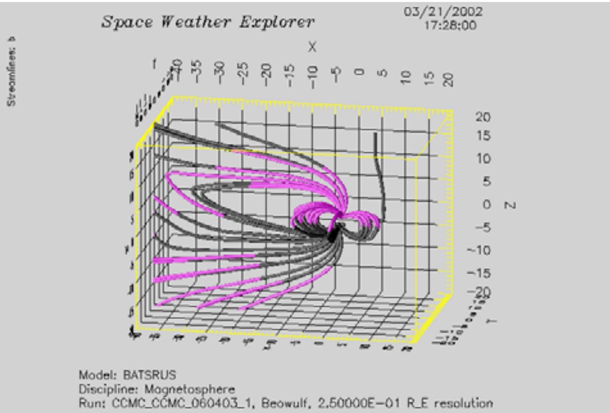

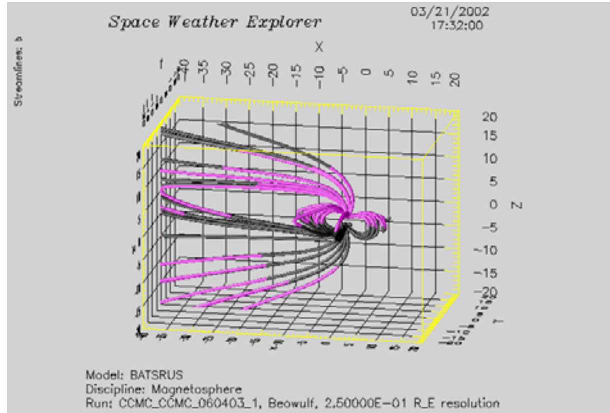

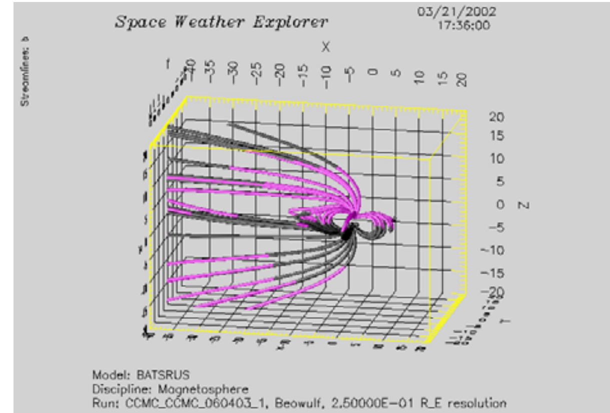

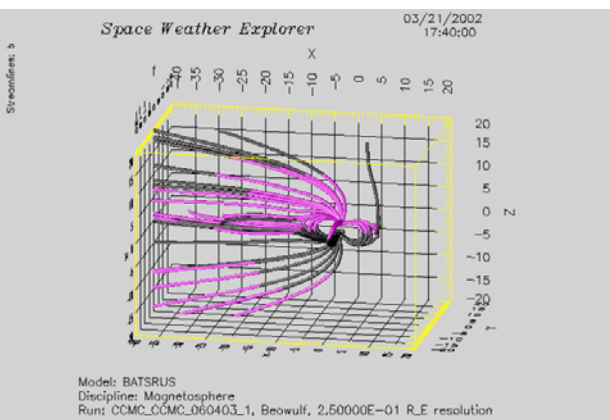

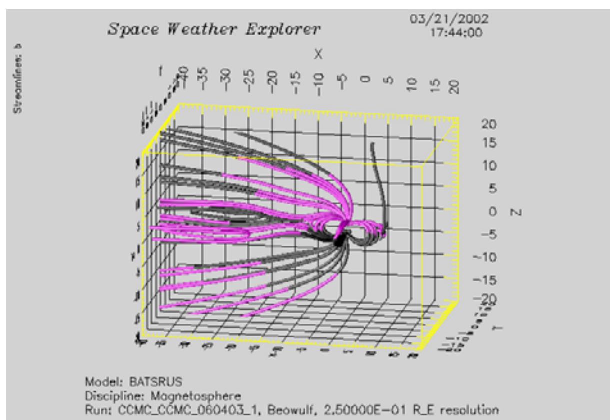

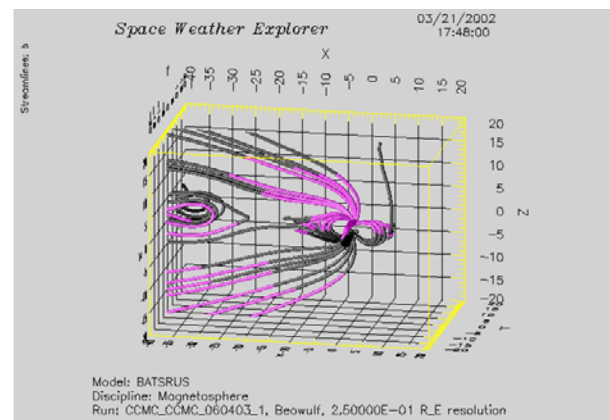

Ring Current Case 1

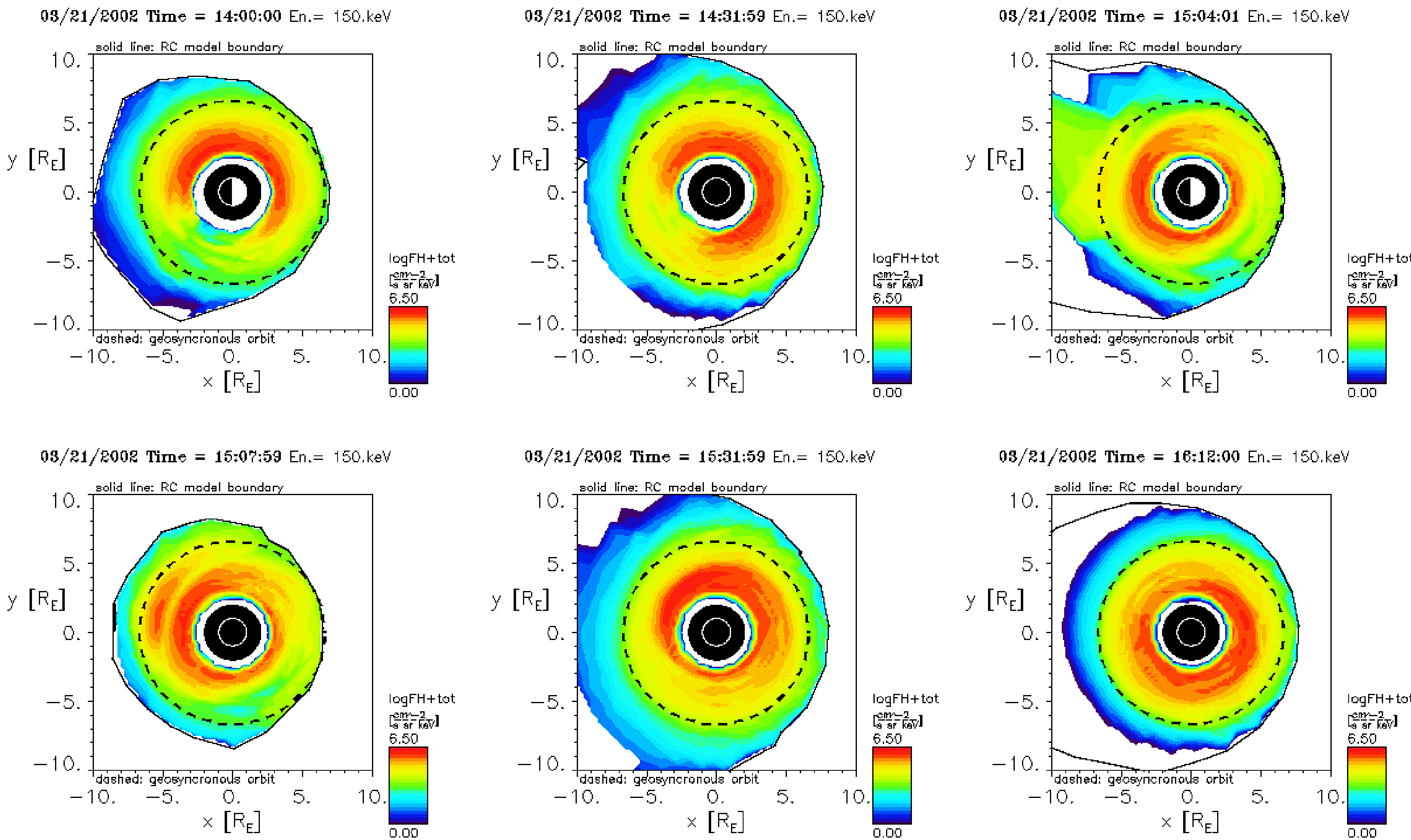

Ring Current Case 1

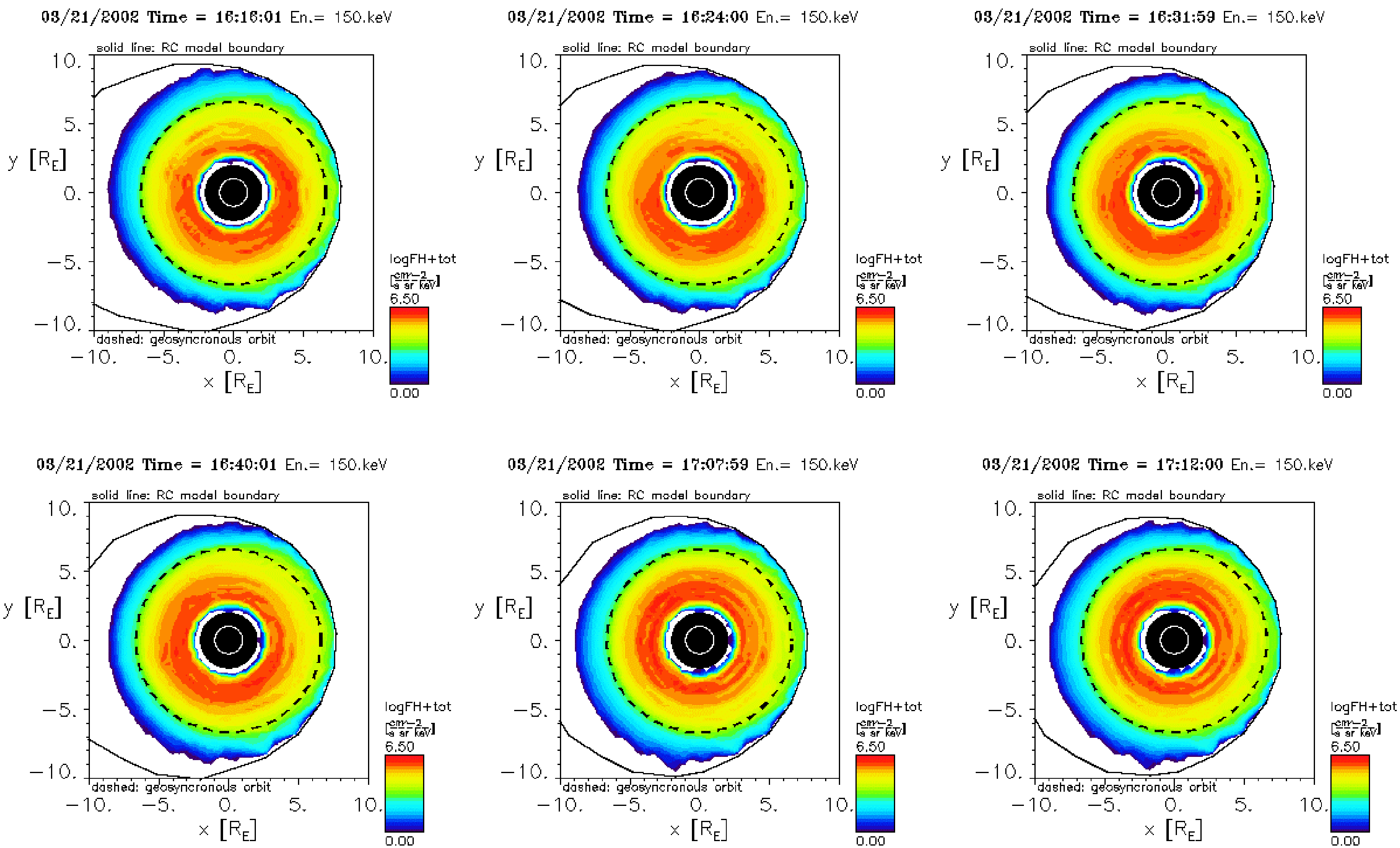

Ring Current Case 1

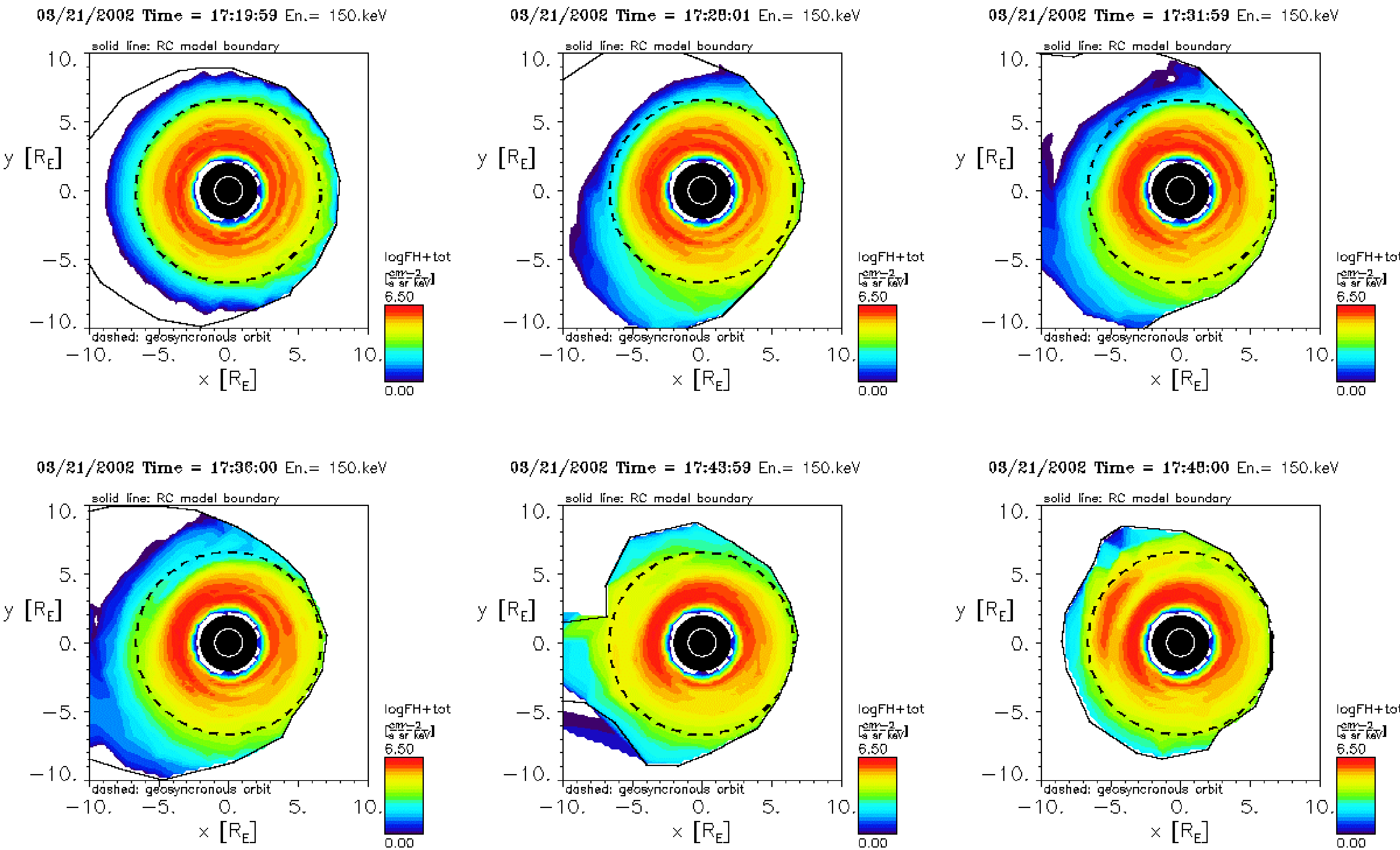

Log (Model Proton Flux) at 21:00 MLT for Case 1 at Geosynchronous Orbit

Log (Model Proton Flux) (#/cm^2/s/sr/keV))

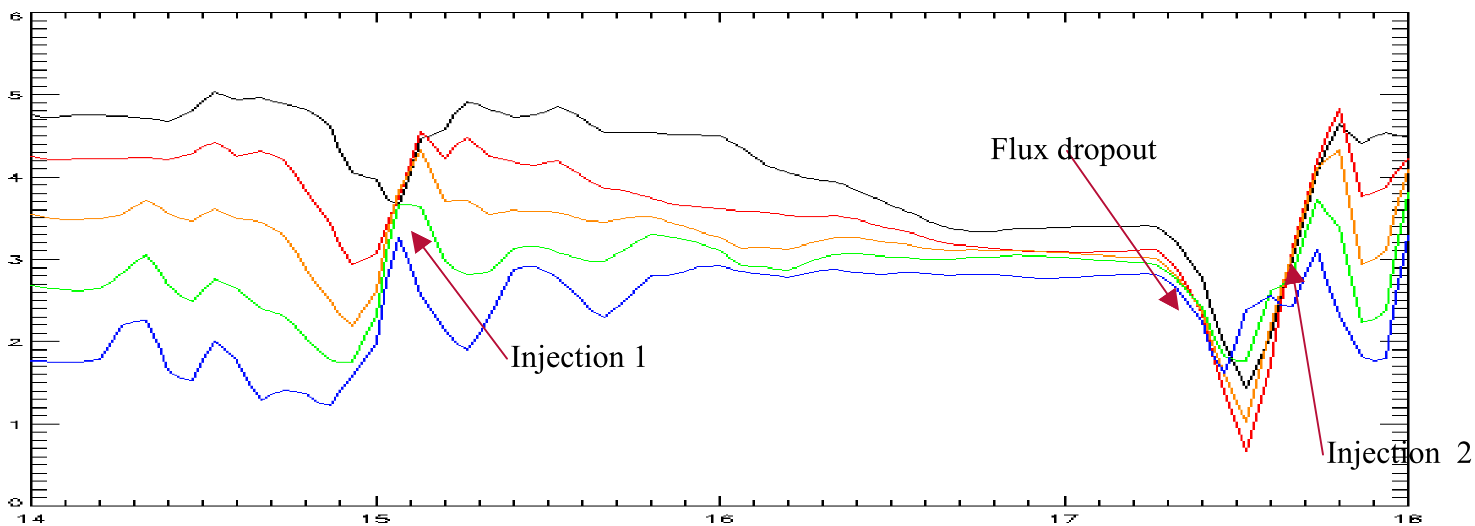

14 15 16 17 18

Universal Time (Hours)

Energies (keV):

62.5 black 94 red 141.5 orange 210 green 300 blue

Timeline for Case 1

- 14:08
  - Northward IMF impacts magnetopause
- 14:16
  - Magnetopause expands outward
- 14:40
  - Southward IMF impacts magnetopause
- 14:48-15:04
  - Potential increase in ionosphere
  - Magnetopause moves inward
  - Tail stretches
  - Decrease of proton flux on the morning side
- 15:04
  - Plasmoid moves tailward
  - Injection at geosynchronous orbit
- 15:08
  - Northward IMF impacts magnetopause
- 15:12
  - Magnetopause starts to expand outwards
- 15:32
  - Asymmetric ring current (150 keV)

Timeline for Case 1

- 16:00
  - Proton flux increases on the morning side
  - Ring current starts to become more symmetric
- 17:08
  - Southward IMF impacts magnetopause
- 17:20
  - Potential increase in ionosphere
  - Magnetopause moves inward
  - Tail stretches
  - Decrease of proton flux on the morning side
- 17:28
  - Flux dropout in pre-midnight sector
- 17:44
  - Reconnection in tail
  - Injection at geosynchronous orbit
- 17:48
  - Plasmoid moves tailward

➢At 17:28, there is a flux dropout in the premidnight sector (especially in the 90-150 keV energy range). The flux dropout at high energies during growth phase is due to B decrease at this substorm phase. In order to conserve the third adiabatic invariant, ions drift shells expand to higher L and at the same time particles lose energy. This causes the flux dropout.

Run with Model Solar Wind Conditions Case 2

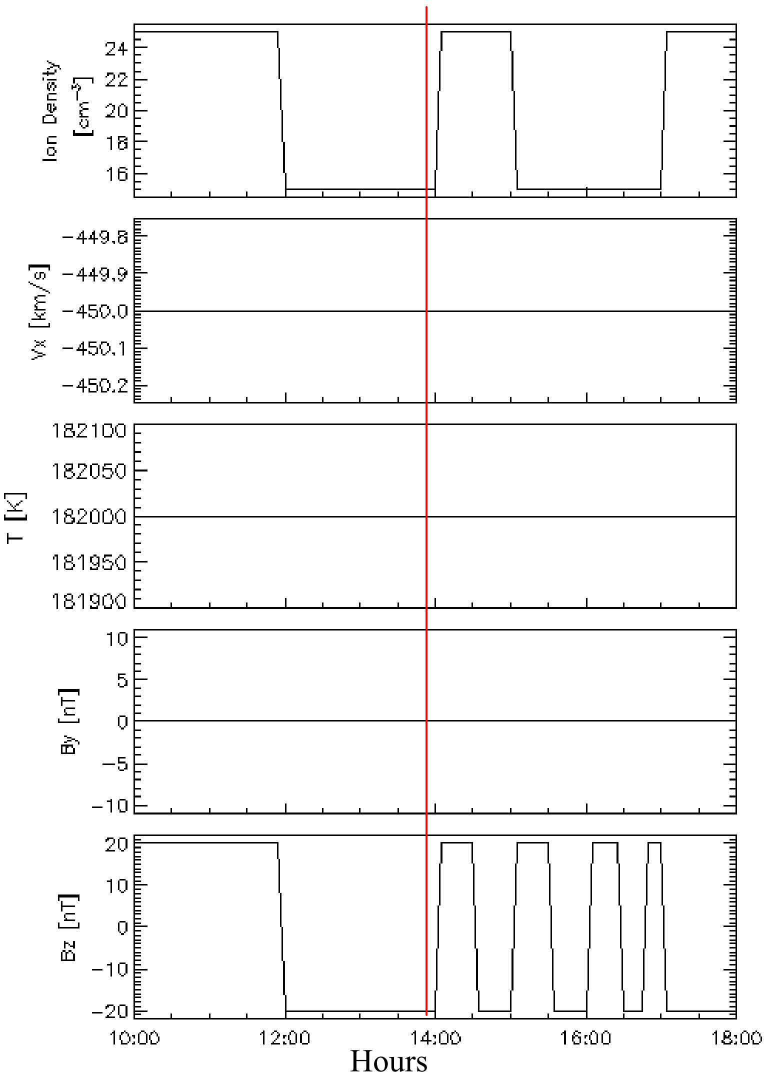

Cross Polar Cap Potential in Northern Hemisphere

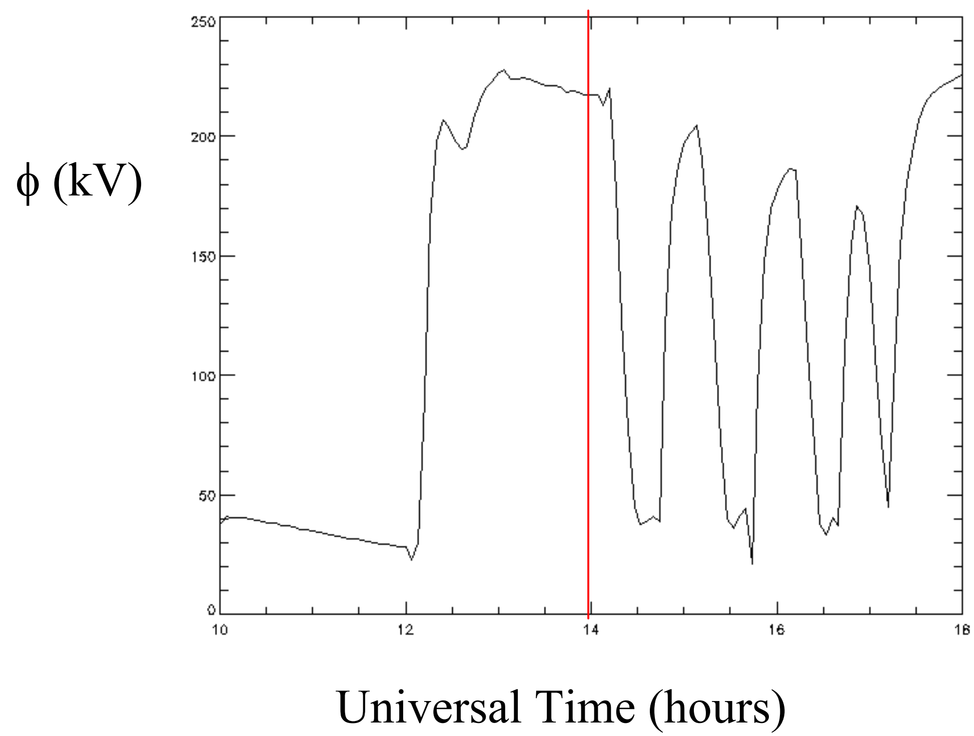

The period before the red line corresponds to a “warm-up” period for the ring current.

Magnetosphere Case 2

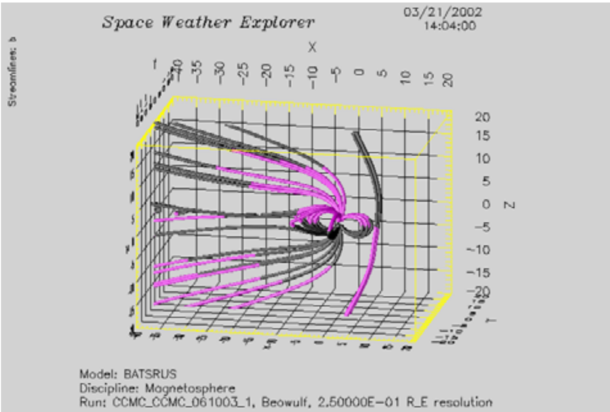

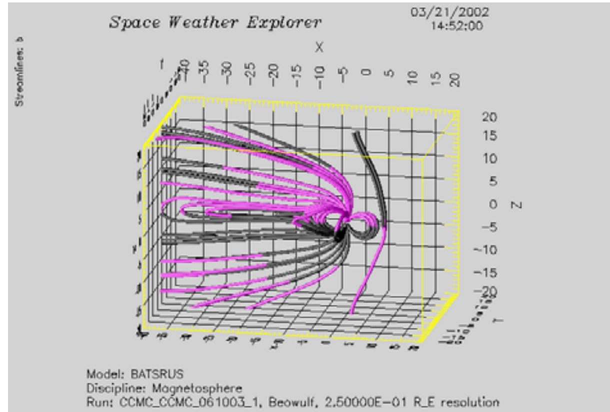

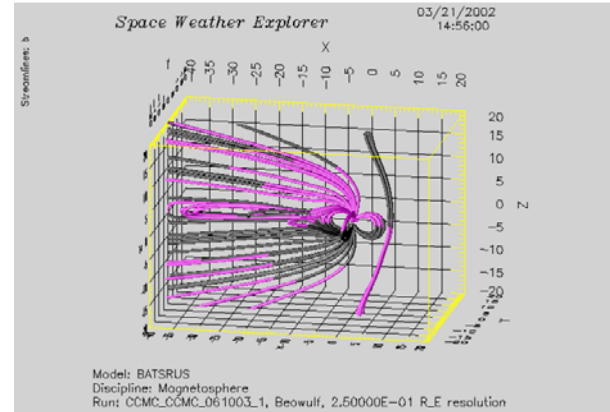

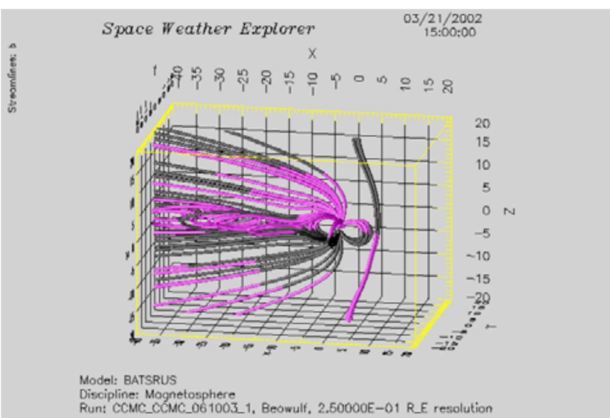

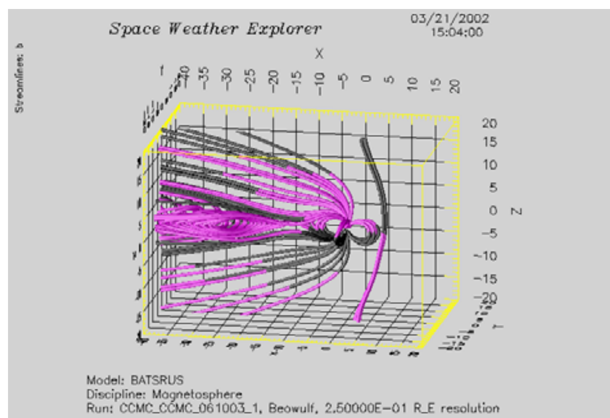

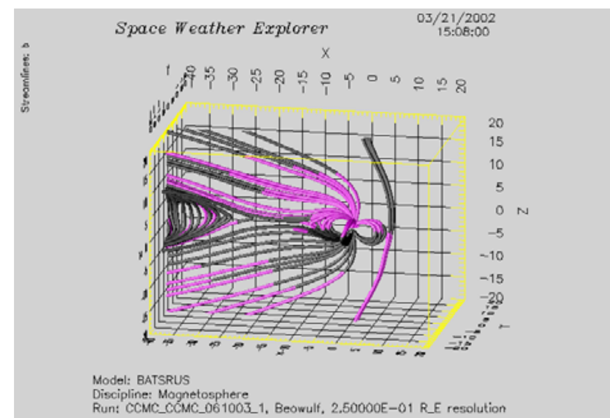

Magnetosphere Case 2

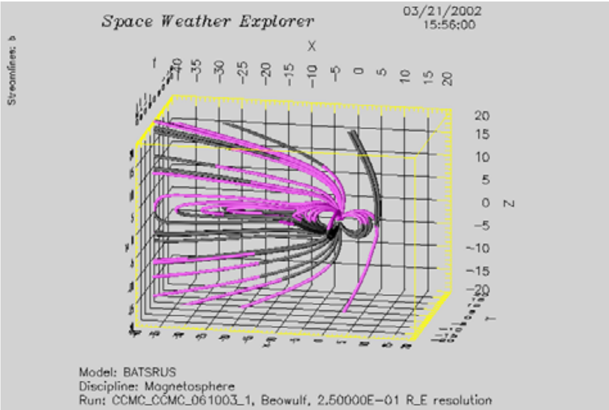

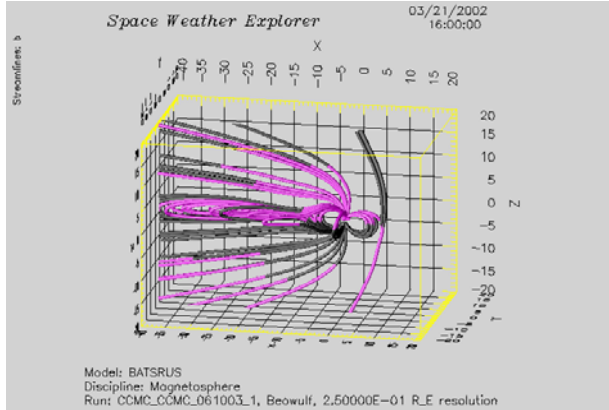

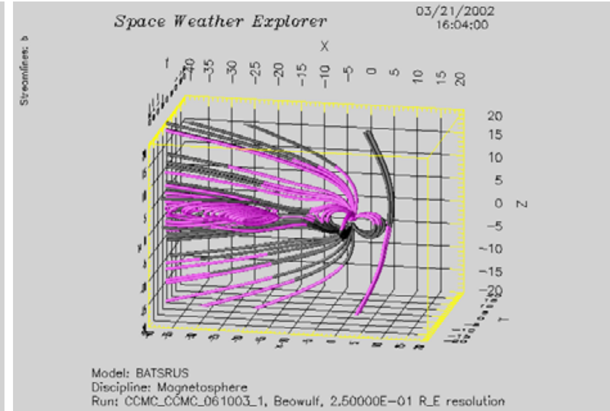

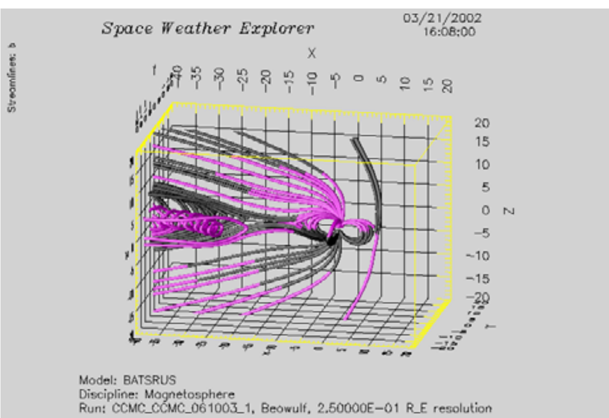

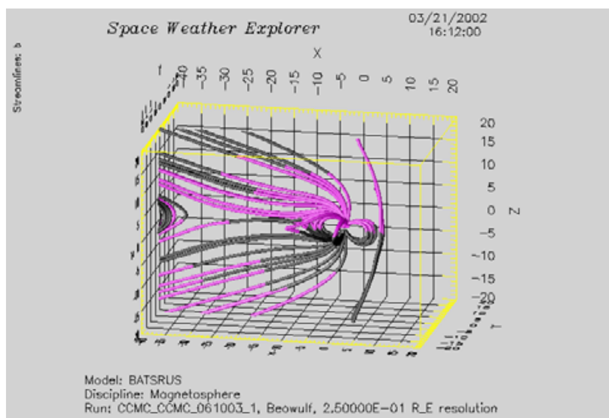

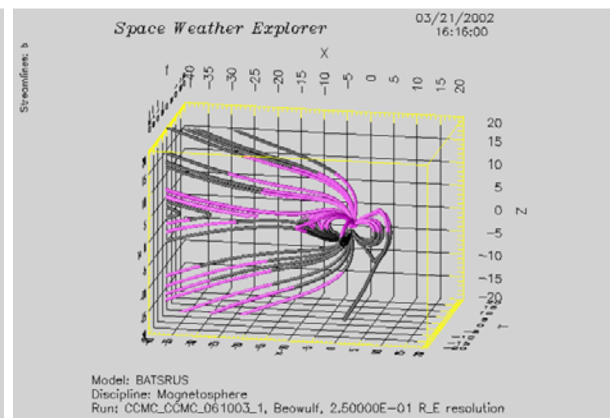

Magnetosphere Case 2

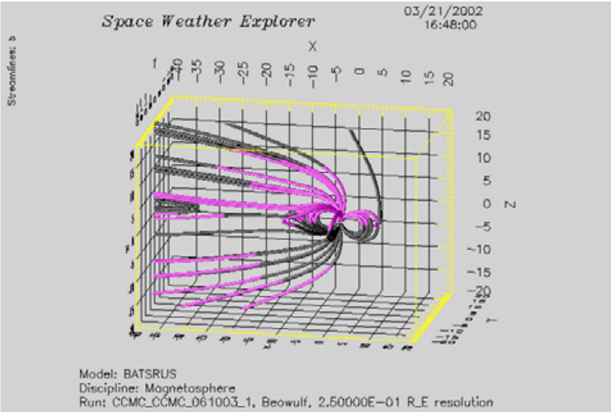

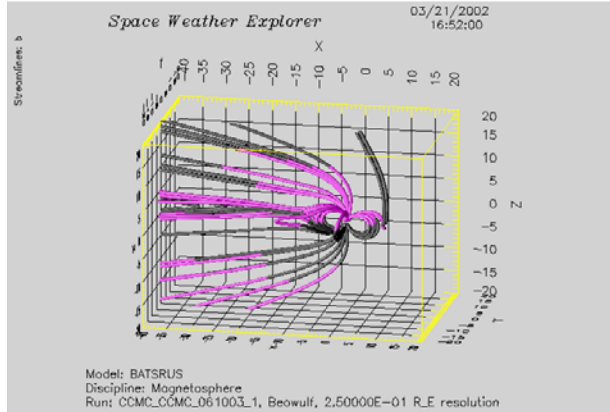

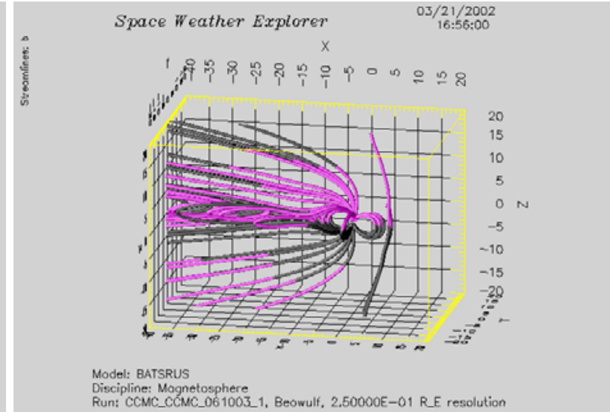

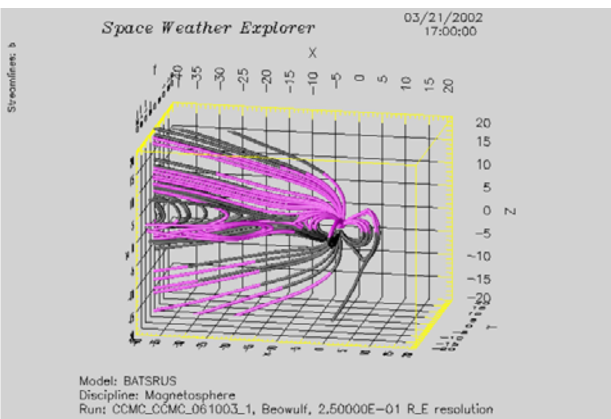

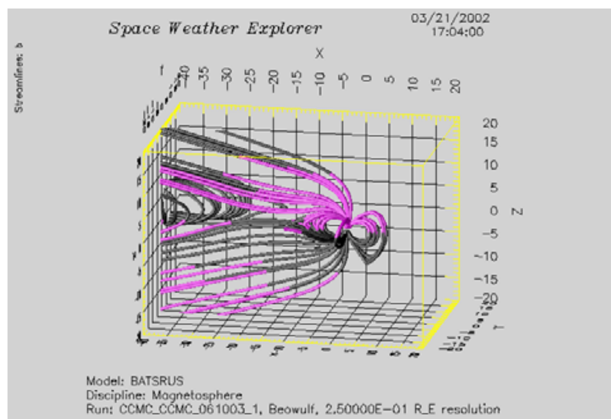

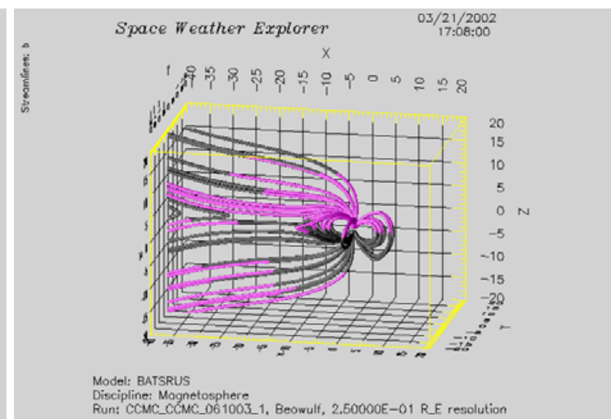

Magnetosphere Case 2

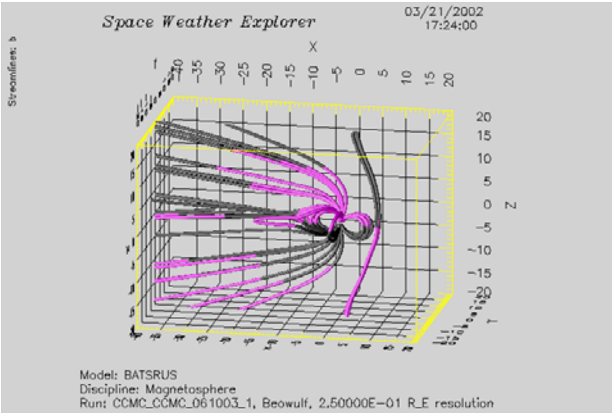

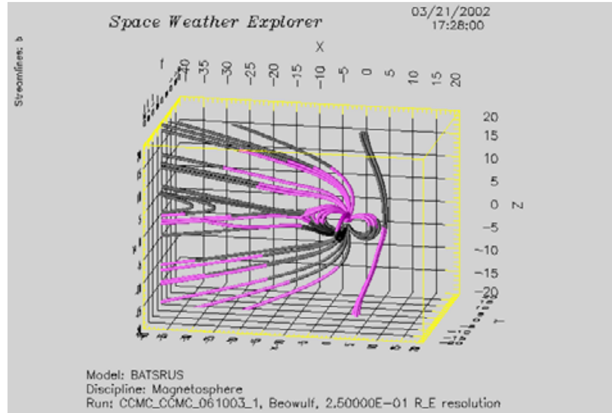

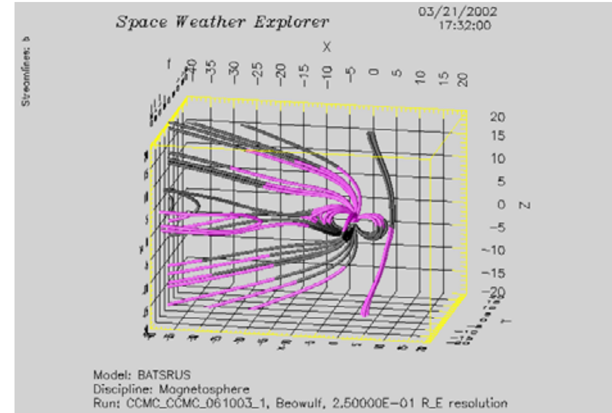

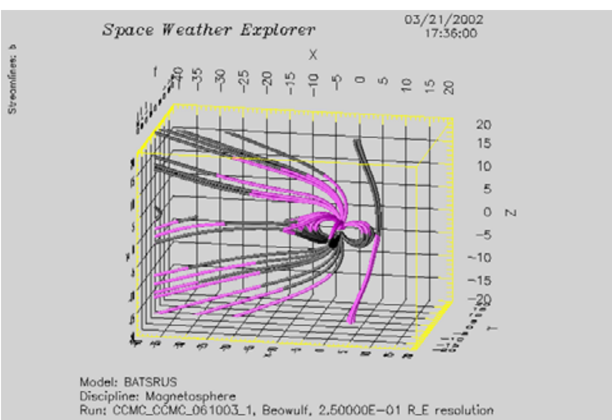

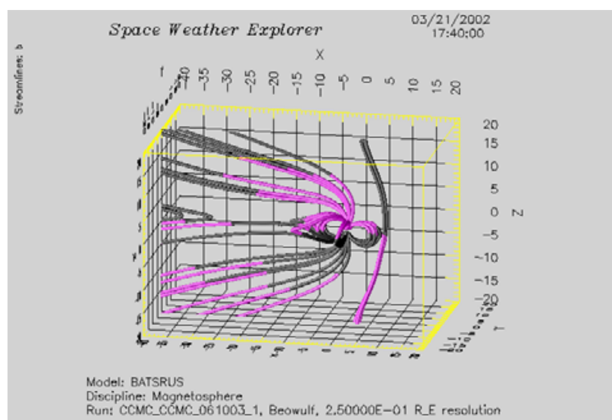

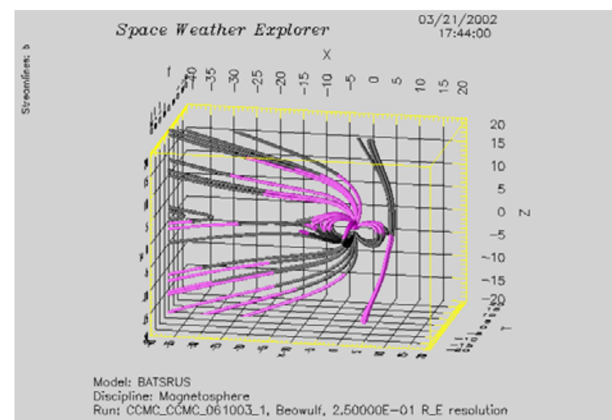

Ring Current Case 2

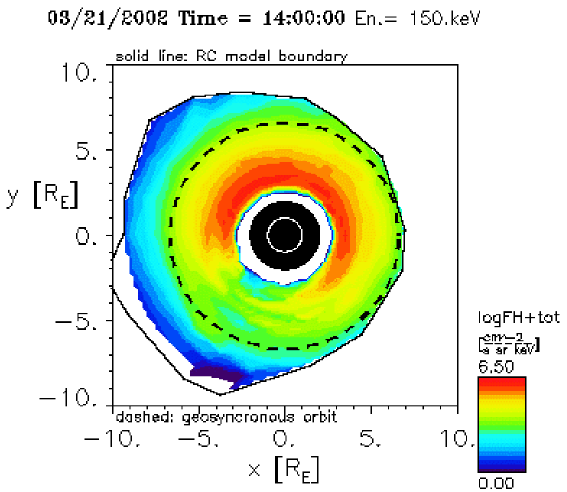

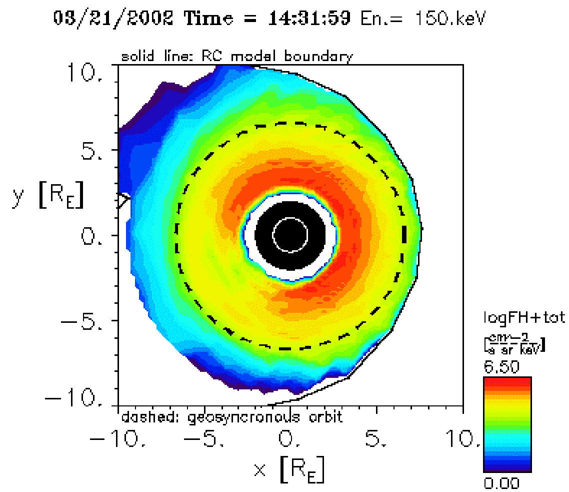

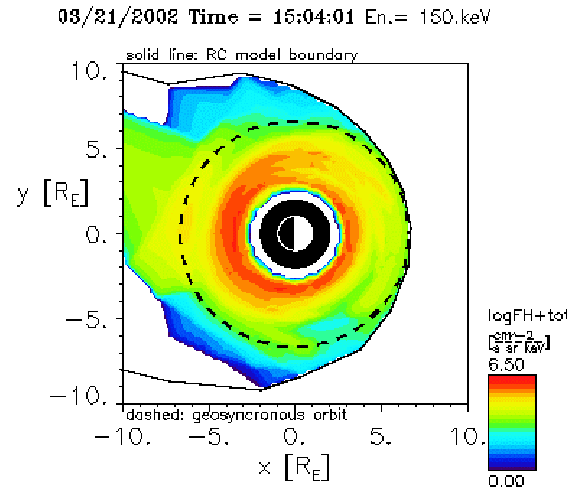

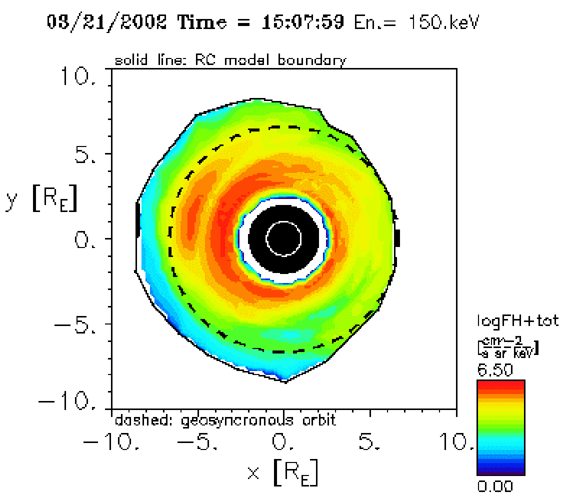

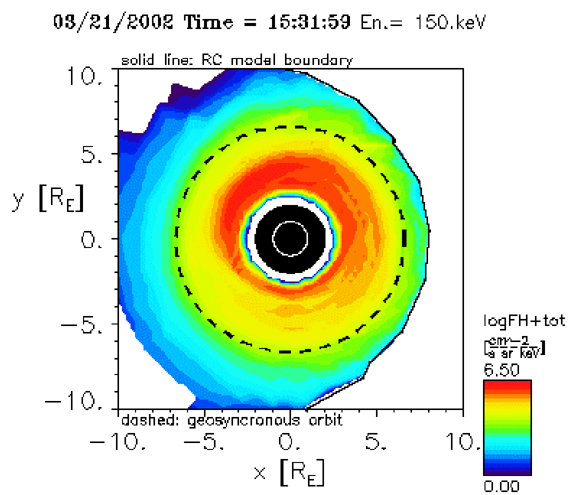

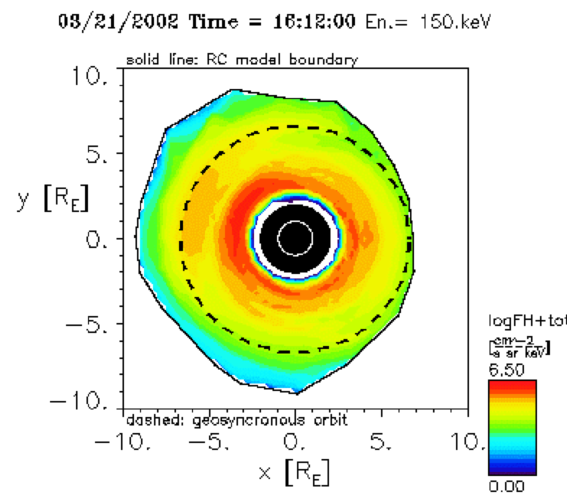

Ring Current Case 2

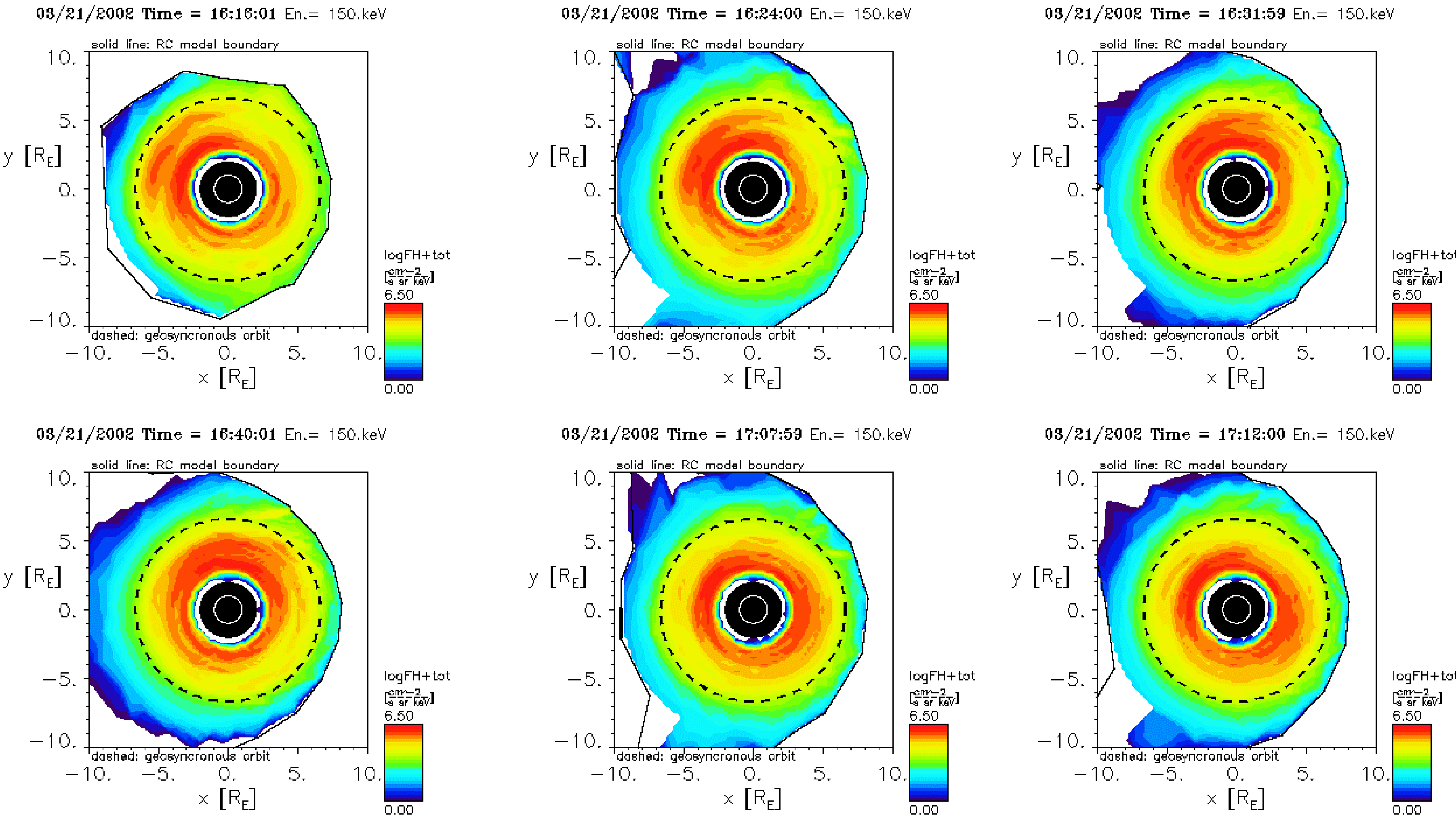

Ring Current Case 2

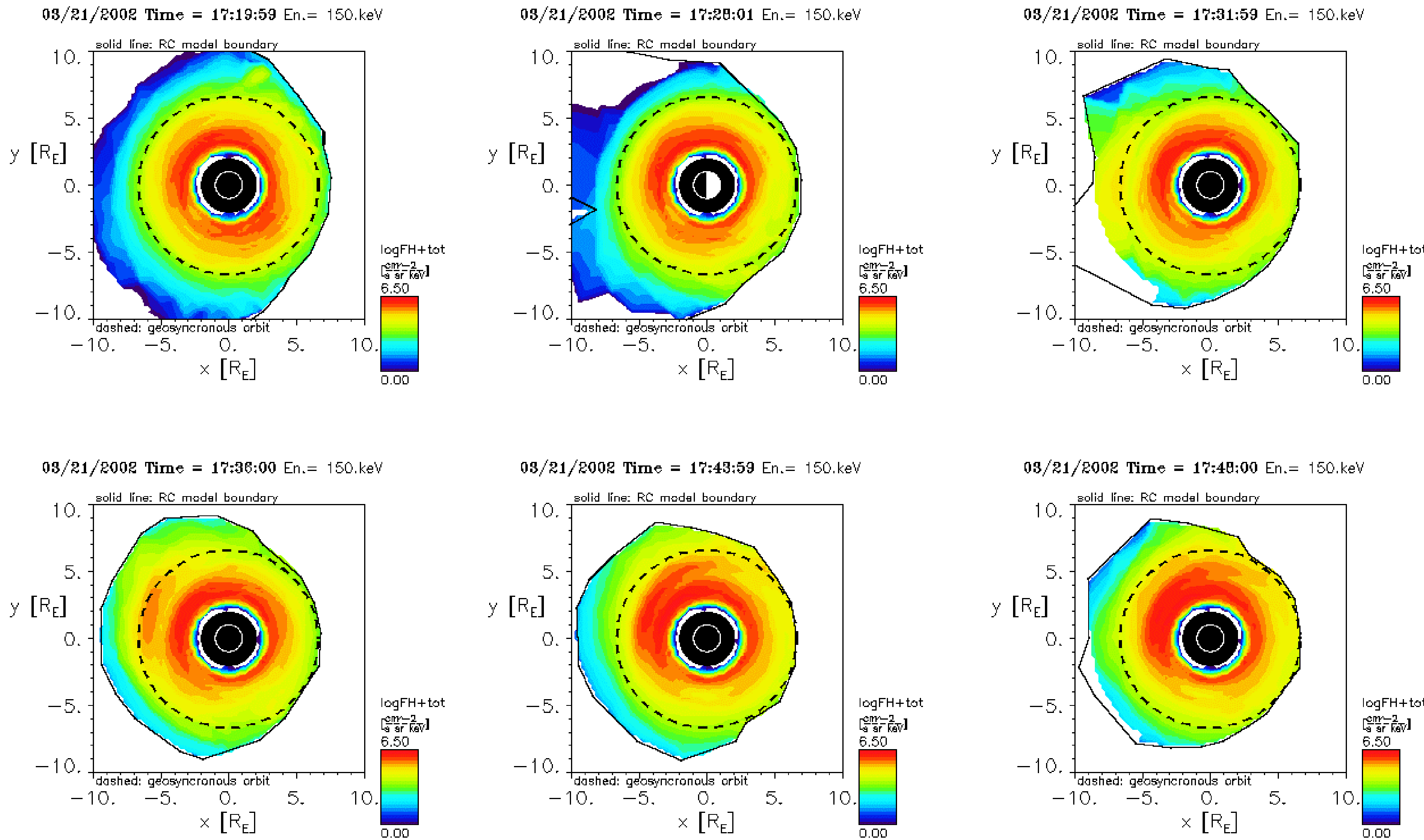

Log (Model Proton Flux) at 21:00 MLT for Case 2 at Geosynchronous Orbit

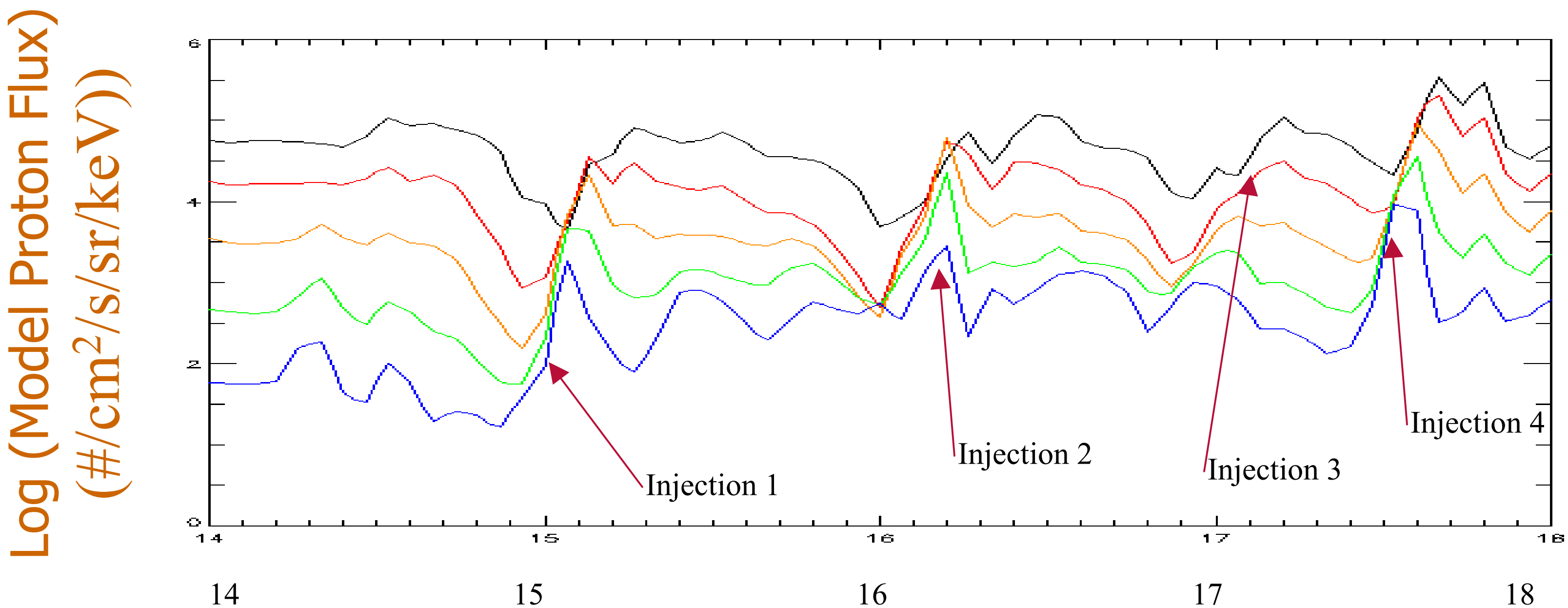

Universal Time (Hours)

Energies (keV):

62.5 black 94 red 141.5 orange 210 green 300 blue

Timeline for Case 2

- 14:08
  - Northward IMF impacts magnetopause
- 14:16
  - Magnetopause expands outward
- 14:40
  - Southward IMF impacts magnetopause
- 14:48-15:04
  - Potential increase in ionosphere
  - Magnetopause moves inward
  - Tail stretches
  - Decrease of proton flux on the morning side
- 15:04
  - Plasmoid moves tailward
  - Injection occurs at geosynchronous orbit
- 15:08
  - Northward IMF impacts magnetopause
- 15:12
  - Magnetopause starts to expand outwards
- 15:32
  - Asymmetric ring current (150 keV)

Timeline for Case 2

- 15:38
  - Southward IMF impacts magnetopause
- 15:44
  - Potential increase in ionosphere
  - Magnetopause moves inward
- 15:48
  - Tail stretches
  - Proton flux starts to decrease on morning side (smaller decrease than at 14:48)
- 16:04
  - Plasmoid moves tailward
- 16:08
  - Northward IMF impacts magnetopause
- 16:12
  - Magnetopause starts to expand outwards
  - Injection occurs at geosynchronous orbit
- 16:34
  - Southward IMF impacts magnetopause
- 16:40
  - Potential increase in ionosphere
- 16:44
  - Magnetopause moves inward slightly

Timeline for Case 2

- 16:52
  - Tail stretches
  - Northward IMF impacts magnetopause
- 16:56
  - Plasmoid moves tailward
- 17:04
  - Magnetopause starts to expand outwards
- 17:08
  - Small injection inside geosynchronous orbit seen in lower energy (62.5, 94 keV)
  - Southward IMF impacts magnetopause
- 17:12
  - Potential increase in ionosphere
  - Magnetopause moves inward slightly
- 17:20
  - Proton flux decreases on morning side
- 17:24
  - Tail stretches
- 17:32
  - Plasmoid moves tailward
  - Injection at geosynchronous orbit

Discussion

- In case 1, the higher energy fluxes become symmetric between 15:00 and 17:00.
- In case 2, the run is not as symmetric as case 1 between 15:00 and 17:00.
- In case 2, there are more particle injections than case 1 and the particle injections tended to occur shortly after a plasmoid being released down the tail.
- In case 1, a flux dropout occurs around 17:28. There was no flux dropout in case 2.
- In case 2, the second and third particle injections are smaller than the first particle injection. At the time of the injections, the density at 10 R_E is smaller.

Energy in the Ring Current

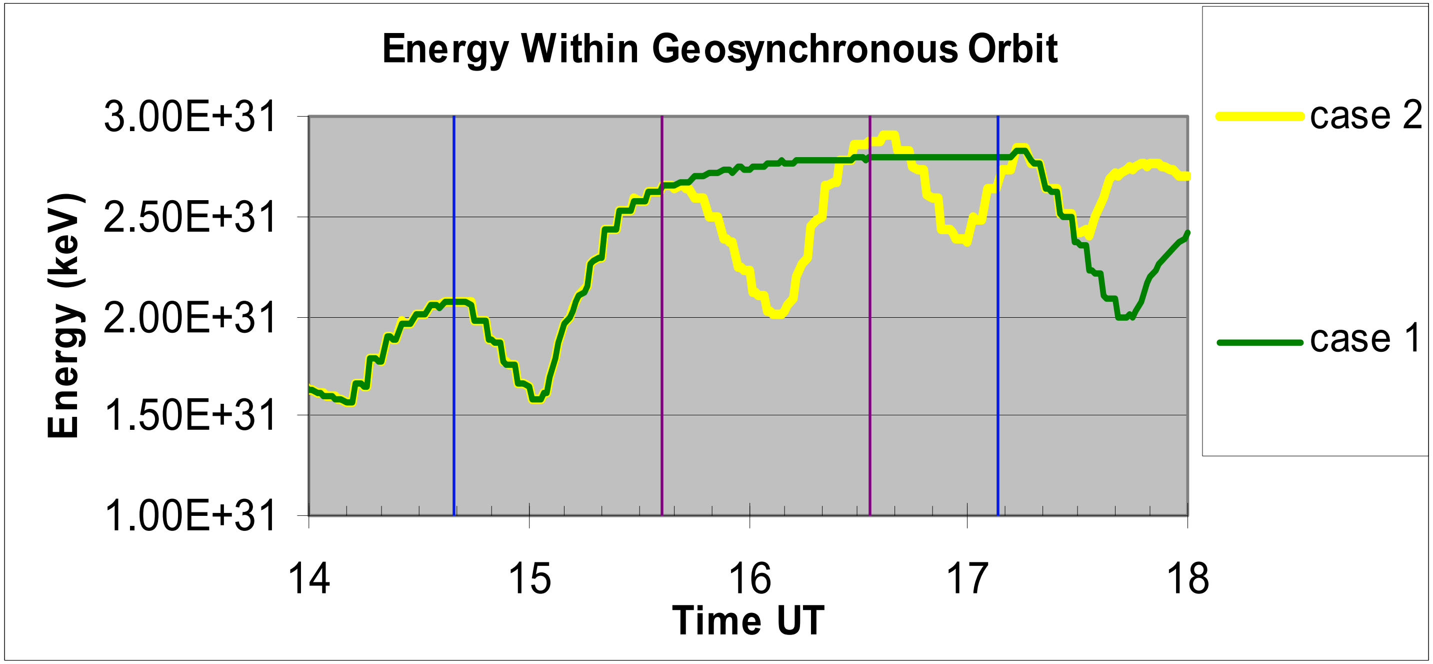

The blue line shows the approximate times that the southward IMF hits the magnetopause for both case 1 and case 2. The purple line shows the approximate times that the southward IMF hits the magnetopause for case 2. The green line shows the energy within geosynchronous orbit for case 1. Injections in the ring current occur around 15:04 and 17:44. These times correspond to the second and third increases in the energy for the ring current. The yellow line shows case 2. Injections occurred around 15:04, 16:12, 17:08 and 17:32. These times correspond to the last four increases in energy in the ring current for case 2. In case 2, the increases in energy are smaller for injections that occurred around 16:12 and 17:08. During the time from 15:00 to 17:00 the solar wind density was constant. After 17:00, the solar wind density was increased.

Losses out the Dayside

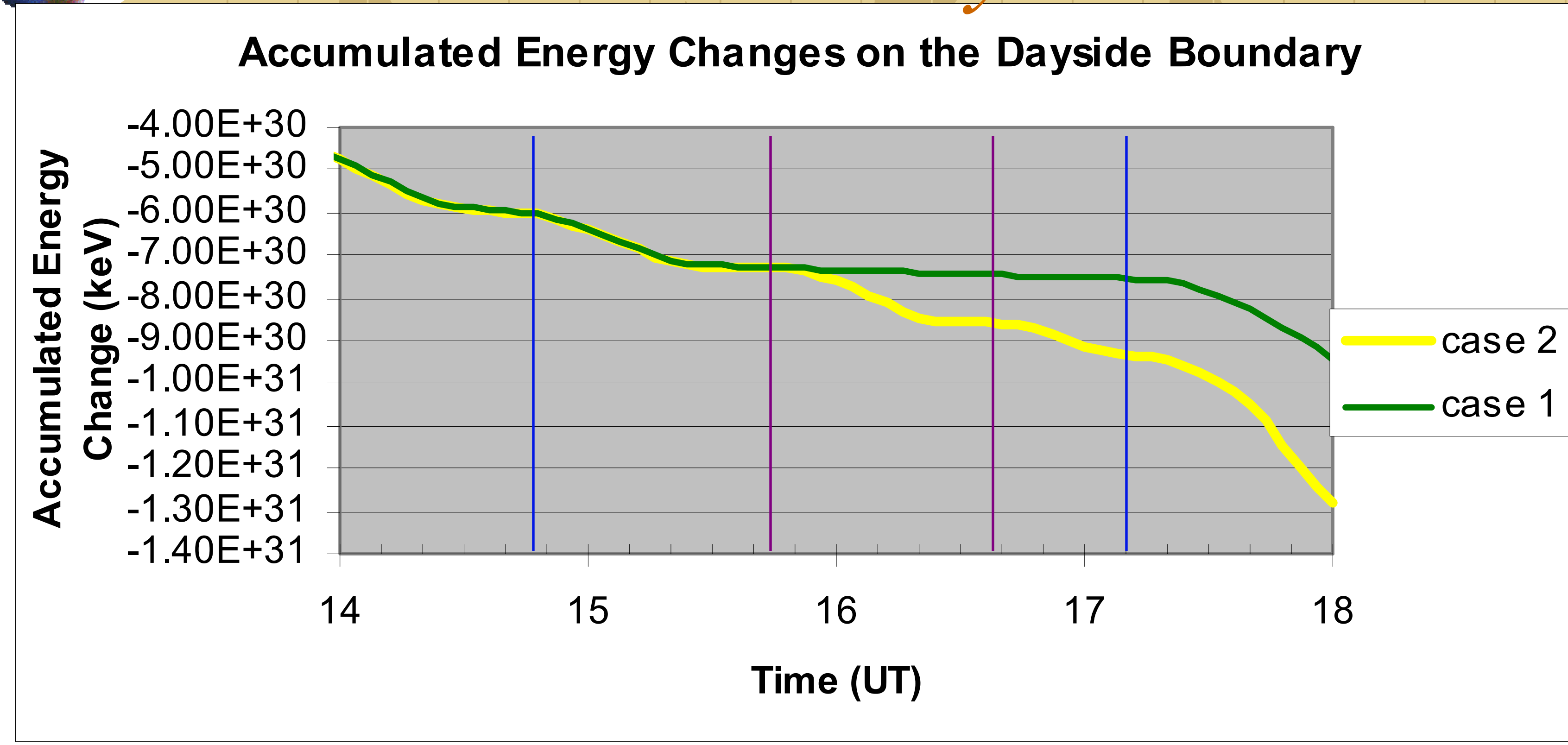

This is a plot of the accumulated energy change for the dayside boundary. The slope of the curve indicates where losses occur. Whenever the curve is flat, there are no additional losses or gains in energy. The blue line shows the approximate times that the southward IMF hits the magnetopause for both case 1 and case 2. The purple line shows the approximate times that the southward IMF hits the magnetopause for case 2.

There are large losses on the dayside approximately 12 minutes after the IMF turns southward. Approximately 6-8 minutes after the southward turning, the potential starts to increase and the magnetopause moves inward on the dayside. When the IMF turns southward for the first three times, the solar wind dynamic pressure is kept constant. Reconnection on the dayside causes the open/closed field boundary to move closer to the Earth. Case 2 has a larger loss after 17:40. The potential for case 2 is slightly higher than case 1 from 17:20 onwards.

Nightside

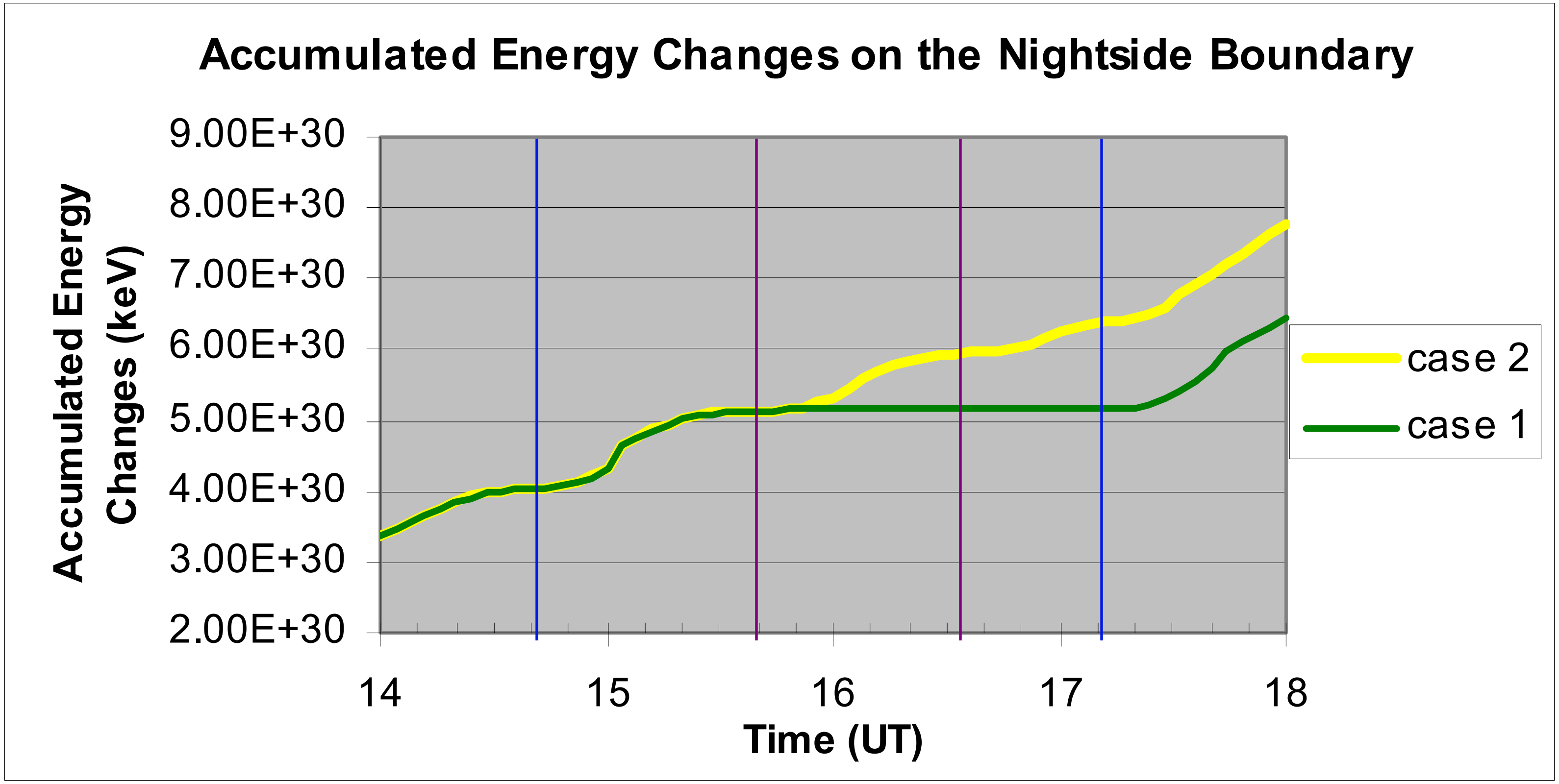

This is a plot of the accumulated energy change for the nightside boundary. The slope of the curve indicates where gains occur. Whenever the curve is flat, there are no additional losses or gains in energy. The blue line shows the approximate times that the southward IMF hits the magnetopause for both case 1 and case 2. The purple line shows the approximate times that the southward IMF hits the magnetopause for case 2.

There are large increases on the nightside approximately 12 minutes after the IMF turns southward. Approximately 6-8 minutes after the southward turning, the potential starts to increase. The increases in energy on the nightside boundary correspond to the losses on the dayside. The increases in energy on the nightside are slightly smaller than the decreases on the dayside boundary. These changes are not enough to account for the changes in energy.

Energy Changes due to Drift

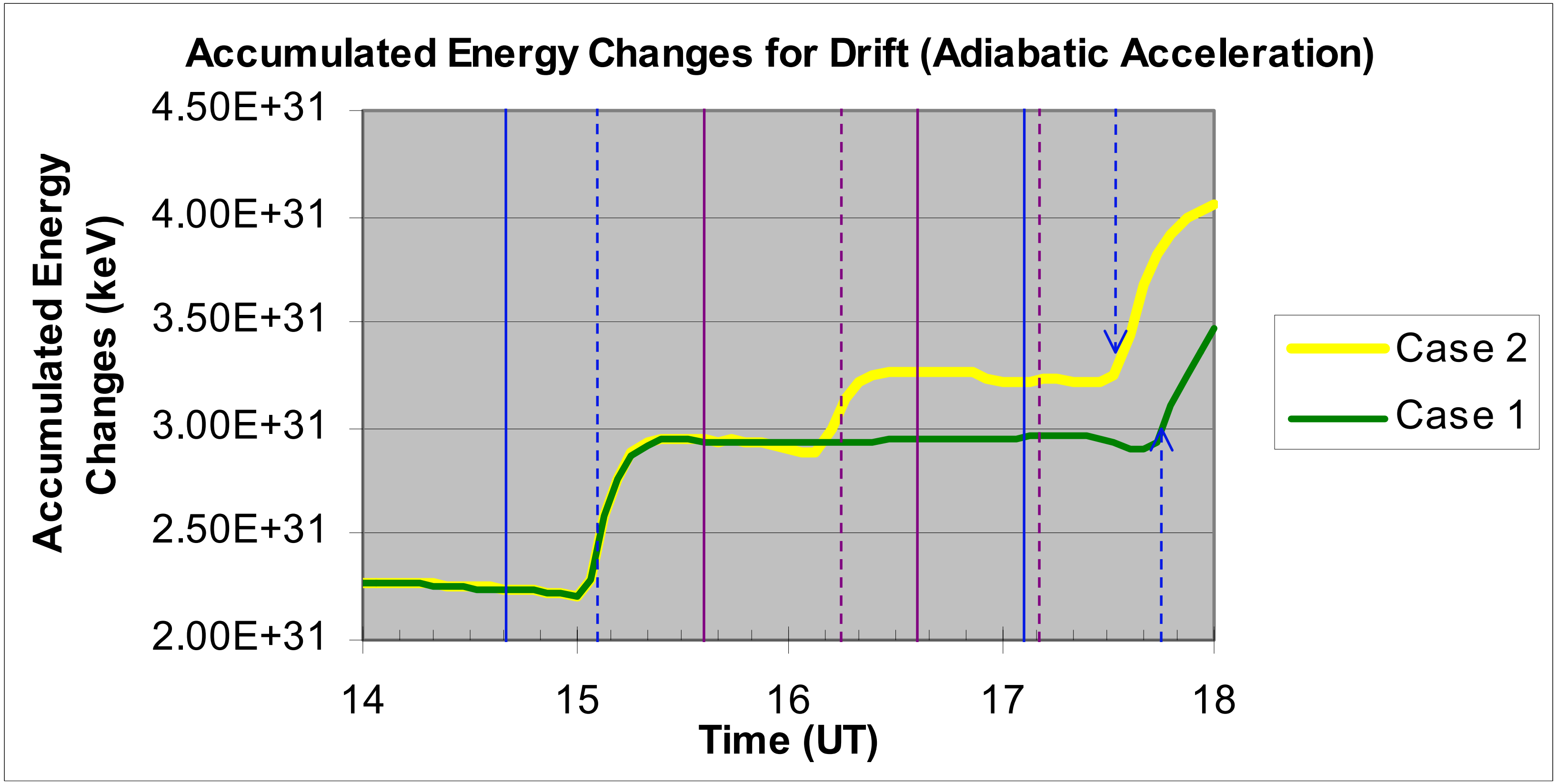

This is a plot of the accumulated energy change due to the drift terms. This acceleration is due to an increase in convection. As convection is increased, particles are pushed toward the Earth. The slope of the curve indicates where gains occur. Whenever the curve is flat, there are no additional losses or gains in energy. The blue line shows the approximate times that the southward IMF hits the magnetopause for both case 1 and case 2. The blue dashed line shows the approximate times where injections occur for both case 1 and case 2. The purple line shows the approximate times that the southward IMF hits the magnetopause for case 2. The purple dashed line shows the approximate times where injections occur for for case 2.

Increases occur around the time reconnection occurs in the tail. There is no increase for the third injection in case 2. This injection was very small. The time period corresponds to the lowest increase in ionospheric potential and density in the tail.

Energy Changes due to Charge Exchange

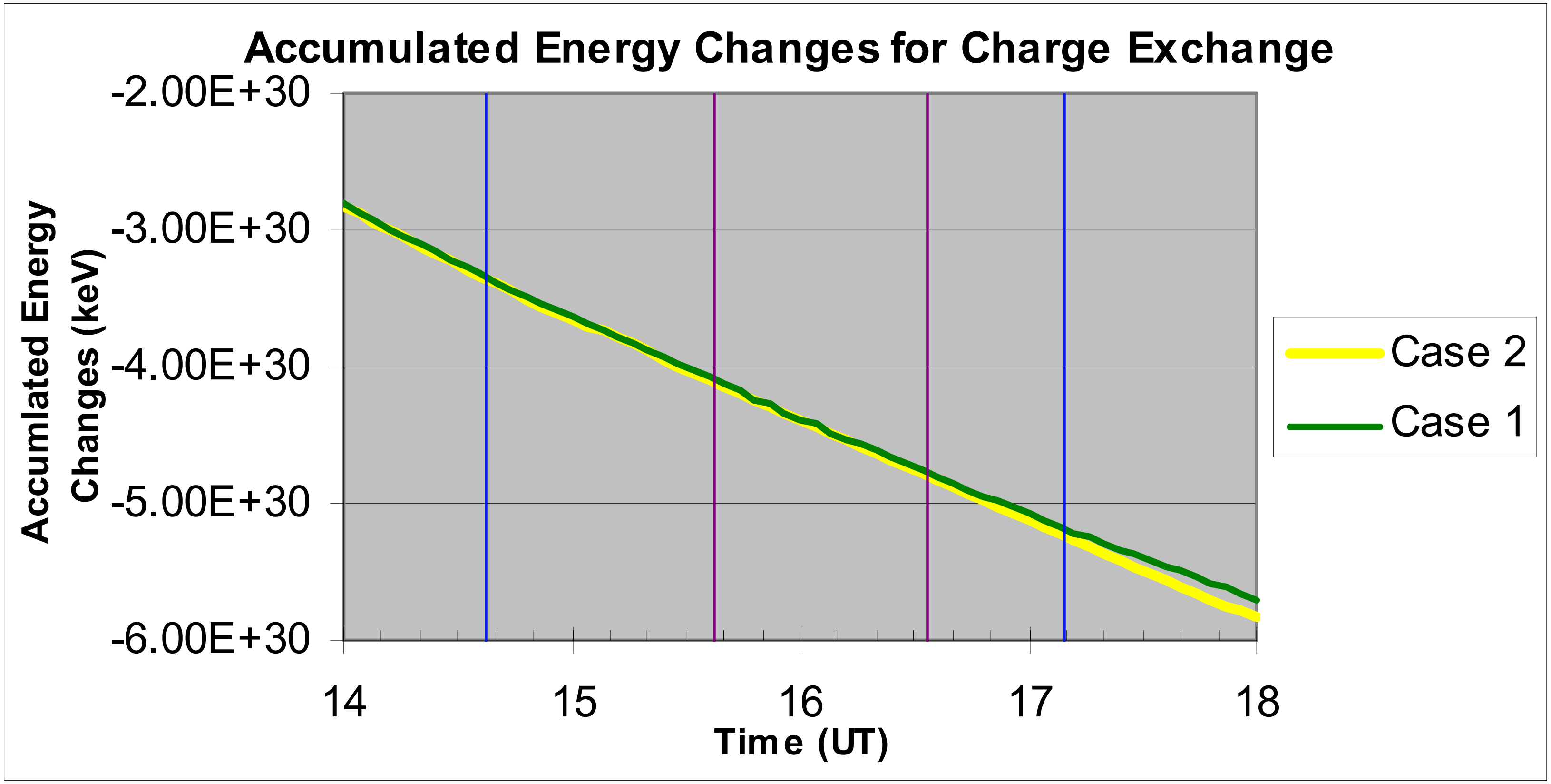

This is a plot of the accumulated energy change due to charge exchange. The slope of the curve indicates where gains occur. Whenever the curve is flat, there are no additional losses or gains in energy. The blue line shows the approximate times that the southward IMF hits the magnetopause for both case 1 and case 2. The purple line shows the approximate times that the southward IMF hits the magnetopause for case 2.

There are only small differences in the two cases and the loss is fairly constant. This term does not account for the oscillations in the energy.

Energy Changes due to Changing B

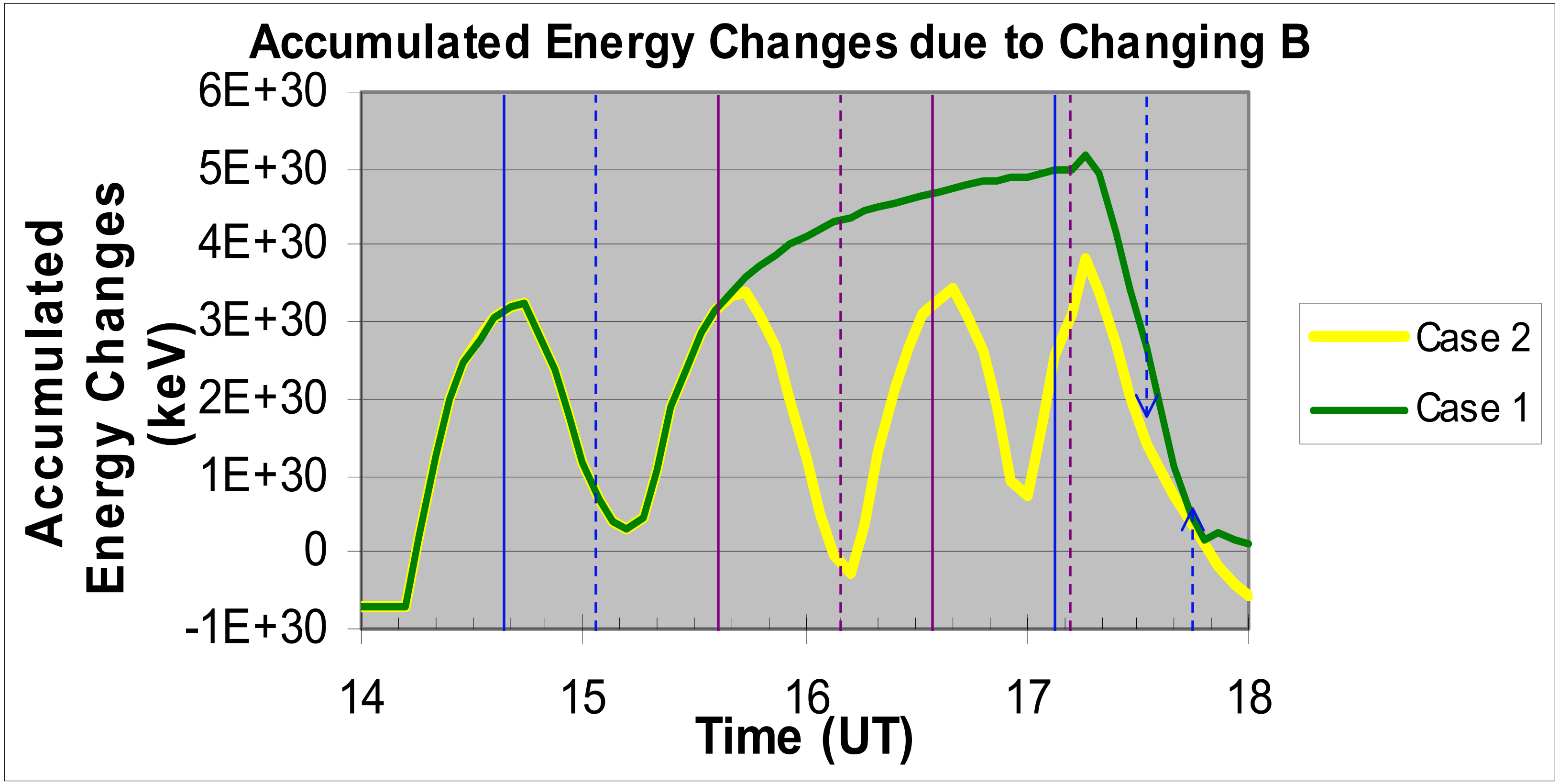

This is a plot of the accumulated energy change due to the changing B. This term assumes that the first and second adiabatic invariant are conserved. Changes in B then change the kinetic energy. The slope of the curve indicates where gains occur. Whenever the curve is flat, there are no additional losses or gains in energy. The blue line shows the approximate times that the southward IMF hits the magnetopause for both case 1 and case 2. The blue dashed line shows the approximate times where injections occur for both case 1 and case 2. The purple line shows the approximate times that the southward IMF hits the magnetopause for case 2. The purple dashed line shows the approximate times where injections occur for for case 2.

When dipolarization occurs, the energy increases. When the IMF turns southward, the magnetic field stretches and energy is lost.

Summary

- Multiple substorms cause more injections into the ring current but do not cause a significant gain in energy at the end of a cycle.
- During multiple substorms, the ring current is more asymmetric with significant losses on the dayside causing decreases in the proton flux on the morning side.
- During multiple substorms, there is an oscillation in the energy. Energy is lost when the tail stretches during southward IMF. Energy is gained due to dipolarization in the tail and increases in ionospheric potential.

References

- Powell K. G., P. L. Roe, T. J. Linde, T. I. Gombosi, and D. L. De Zeeuw, A solution-adaptive upwind scheme for ideal magnetohydrodynamics, *J. Comput. Phys*., 154(2), 284-309, 1999.
- Fok M.-C., T. E. Moore, and M. E. Greenspan, Ring current development during storm main phase, *J. Geophys. Res., 101,* 15,311-15,322, 1996.
- Fok M.-C., and T. E. Moore, Ring current modeling in a realistic magnetic field configuration, *Geophys. Res. Lett., 24,1775-1778*, 1997.
- Fok M.-C., T. E. Moore, and D. C. Delcourt, Modeling of inner plasma sheet and ring current during substorms, *J. Geophys. Res., 104,* 14,557-14,569, 1999.